

## Evaluation of Silver Nanoparticles Interaction with Melittin and antibiotics on Bacterial Isolates from diarrhea infection patients.

### Abstract:

This study aimed to evaluate the efficiency of Silver nanoparticles (Ag-NPs) and Melittin against *Escherichia coli* and *Staphylococcus aureus* isolates as causes of diarrhea. Silver Nanoparticles (Ag-NPs) characterization using Ultraviolet-visible spectroscopy showed two absorption peaks for the cinnamon bark extract at (220, and 312) nm and 428 nm for the bio-synthesized nanomaterials, which is evidence of the formation of Ag-NPs. Transmission electron microscopy (TEM) showed the shape of the silver nanoparticles and an average size of 22.8 nm, and X-Ray diffraction (XRD) examination to clarify the crystalline properties of Ag-NPs. The Ag-NPs and Melittin showed antimicrobial activity by determining the minimum inhibitory concentration (MIC) and impregnating them with the tested antibiotic discs that were ineffective against bacterial isolates. It was found that there was a partial synergism between Ag-NPs and Melittin with ceftriaxone and ciprofloxacin for *E. coli* and and with vancomycin and tetracycline for *S. aureus* and *E. faecalis*. The synergism between Ag-NPs and Melittin by checkerboard assay showed an apparent synergism between them against all isolates selected for the study.

### تقييم فاعلية جسيمات الفضة النانوية والملتين مع المضادات الحيوية ضد البكتريا المعزولة من المرضى المصابين بالإسهال

كركز محمد ثلج  
جامعة تكريت/ كلية الزراعة

يوسف مليك عطية  
الجامعة العراقية/ كلية التربية/ قسم علوم الحياة

### مستخلص:

هدفت هذه الدراسة إلى تقييم كفاءة جسيمات الفضة النانوية والملتين ضد عزلات *Staphylococcus aureus* و *Escherichia coli* كسببات للإسهال. أظهر توصيف جسيمات الفضة النانوية (Ag-NPs) باستخدام التحليل الطيفي المرئي للأشعة فوق البنفسجية ذروتي امتصاص لمستخلص لحاء القرفة عند (220، و 312) نانومتر و 428 نانومتر للمواد النانوية المصنعة حيويًا، وهو دليل على تكوين جزيئات الفضة النانوية (Ag-NPs). أظهر المجهر الإلكتروني النافذ (TEM) شكل جسيمات الفضة النانوية وبمتوسط حجم 22.8 نانومتر، كما تم فحص حيود الأشعة السينية (XRD) لتوضيح الخواص البلورية لحبيبات الفضة النانوية. أظهر كل من حبيبات الفضة النانوية وبتيد الملتين نشاطًا مضادًا للميكروبات من خلال تحديد التركيز المثبط الأدنى، بالإضافة إلى تشريبها بأقراص المضادات الحيوية المختبرة والتي أبدت العزلات البكتيرية مقاومة ضدها، وقد بينت النتائج وجد أن هناك تآزر جزئي لحبيبات الفضة النانوية والملتين مع السيفترياكسون والسيبروفلو كساسين بالنسبة لبكتريا *E. coli* ومع الفانكوميسين والتتراسيكلين بالنسبة لبكتريا *S. aureus*. أظهرت النتائج حالة التآزر بين حبيبات الفضة النانوية والملتين باستخدام طريقة رقعة الشطرنج ضد جميع العزلات المختارة للدراسة.

### Introduction:

Diarrhea is described as an increase in bowel motions to more than three times per day or a decrease in the quantity of stool firmness (to the point where it is liquid or semi-liquid), both of which are accompanied by clinical symptoms such as fever, vomiting, nausea, and stomach discomfort. (do Nascimento *et al.*, 2022). Statistics issued in 2019 indicated that diarrhea is one of the leading causes of death in more than 500,000 cases worldwide among children under five. (Deichsel *et al.*, 2023).

The main causes of diarrhea include parasites, viruses, and bacteria. Acute and chronic diarrhea are the two categories of diarrhea based on the time of day. Acute diarrhea passes in less than 14 days. It is brought on by a viral or bacterial infection in the stomach. The duration of chronic diarrhea exceeds four weeks. Numerous things may cause it, such as an infection caused by bacteria, viruses, or parasites or a problem with the intestinal tract's functioning components (Chu *et al.*, 2020; Neamah and Merza, 2023). Bacterial infection-related diarrhea is one of the global health problems that

cause infectious diarrhea, especially in developing countries.

Antibiotic resistance has become a major issue in global health as a result of the misuse and overuse of antibiotics, leading to a decrease in effectiveness against bacteria responsible for causing illness (Depta & Niedźwiedzka-Ryśtwej, 2023). Furthermore, one of the factors contributing to the creation of bacterial strains resistant to several antibiotics is the use of antibiotics in the manufacturing of animal and agricultural feed (Singh *et al.*, 2020). According to the World Health Organization (WHO), antimicrobial-resistant bacteria have resulted in the deaths of approximately 541,000 individuals globally, with 133,000 fatalities occurring in Europe (Dey *et al.*, 2023). Finding new therapeutic alternatives other than antibiotics has become an urgent need due to the decreased efforts of most pharmaceutical companies in developing and producing new generations of antibiotics. Developing antibiotics is a complex and expensive process that requires an extended period for approval for their use. Additionally, some antibiotics face restrictions to reduce the emergence of resistance against them (Shrivastava *et al.*, 2018).

Among the contemporary tools used in the biomedical sciences are nanomaterials, particularly silver nanoparticles (Ag-NPs), which help combat various bacterial, viral, and fungal infections and have anti-inflammatory properties (Ribeiro *et al.*, 2023).

Silver nanoparticles (Ag-NPs) may be manufactured using a variety of physical, chemical, and biological processes (S. Singh *et al.*, 2023). The green synthesis technique is widely regarded as a very effective approach for the environmentally conscious manufacturing of nanomaterials. The methodology used many biological sources, including bacteria, fungus, and different plant components, to get extracts rich in diverse active substances such as aliphatic compounds, phenols, alcohols, proteins, and flavone compounds (Parvathalu *et al.*, 2023). This research used an extract derived from the bark of Cinnamon verum, an aromatic plant known for its diverse range of physiologically active chemicals. These compounds have been shown to possess the potential to decrease silver ions and play a crucial role in preserving the integrity and stability of silver nanoparticles during the production process (Alwan & Al-Saeed, 2021).

Melittin is classified as an antimicrobial peptide. The discovery of it can be traced back to 1970. *Apis mellifera* is regarded as the main origin of the Melittin peptide and constitutes around 50% of its total weight when dried. This peptide is cationic and hemolytic, and it has a threadlike structure in aqueous solutions. However, when it encounters biological membranes, it undergoes a shift in shape and forms a helical structure known as an alpha-helix. Melittin is composed of 26 amino acids, and possesses numerous antibacterial, antiviral, and antifungal properties. It is extensively employed in the treatment of diverse ailments affecting different organs and systems of the body, including arthritis, central and peripheral nervous system disorders, skin diseases, cardiac issues, ulcers, colitis, cancer, and diabetes (Hossen *et al.*, 2017; Moridi *et al.*, 2020).

The precise method by which melittin interacts with biofilms remains to be discovered, despite numerous studies and proposals in this field. H.W. Huang's concept is widely regarded as the most valid explanation for the process by which maltin degrades the membranes of live cells. Melittin adheres to the surface of the biological membrane

and then infiltrates the membrane by creating pores, which enables it to disrupt the integrity of the cytoplasmic membrane (Hong *et al.*, 2019).

Typically, the interaction between Melittin and the cytoplasmic membrane can be divided into two distinct stages: the initial stage involves the association of Melittin with the membrane, while the subsequent stage involves the aggregation of peptides. This is followed by the process of guiding and inserting Melittin into the membranes, resulting in the formation of transmembrane pores. The pores generated from the melittin's action are characterized as resembling the toroidal model. During the process of pore creation in membranes, the upper lipid layer bends downwards towards the bottom of the membrane. This causes the walls of the pores to be lined by curved maltin molecules and phospholipids originating from the outside surface of the cytoplasmic membrane (Huang, 2006).

Therefore this research aimed to determine the ability of each of Melittin and Ag-NPs singly or in combination as antimicrobials and evaluate this effectiveness against diarrhea-causing bacterial isolates.

### 3- Materials and methods:

The Stool samples were examined to identify the bacterium causing diarrhea through microscopic analysis. The specimens were cultured on Blood and MacConkey agar. Selective culture media such as Mannitol salt agar were utilized, along with diagnostic biochemical tests like (IMVIC), Urease, Catalase, Oxidase, Kligler, and Coagulase tests, to culture the resulting bacteria. Confirmatory testing was done using the Vitek 2 Compact to identify the specific type of bacteria. The Kirby-Bauer disk diffusion technique was used by spreading a bacterial suspension titrated with ( $1.5 \times 10^8$  CFU/ml) MacFarland's standard turbidity constant with a sterile cotton swab onto a petri dish of Mueller-Hinton agar culture medium (Alhamadani & Oudah, 2022). 8 antibiotics (Maat-Group, UK) were tested, which included Ampicillin ( $10\mu\text{g}$ ), Ceftriaxone ( $30\mu\text{g}$ ), Gentamycin ( $10\mu\text{g}$ ), Amicacin ( $30\mu\text{g}$ ), Ciprofloxacin ( $5\mu\text{g}$ ), Trimethoprim ( $5\mu\text{g}$ ), Tetracycline ( $30\mu\text{g}$ ), Erythromycin ( $15\mu\text{g}$ ) and Vancomycin ( $30\mu\text{g}$ ). The experiment was conducted in a controlled setting when the illumination conditions were intentionally diminished. It added 10 ml of Cinnamom verum extract to 90 ml of silver nitrate solution (1 mM)

at 60 °C, as depicted in Figure 1. The addition was conducted slowly and gradually, with the mixture being continuously stirred for one hour. The visual observation of a dark brown color within the mixture serves as a visual indicator of the successful synthesis of silver nanoparticles (Mariswamy *et al.*, 2021). Various diagnostic tests were performed using diverse methodologies, including

UV-visible spectroscopy, FT-IR, XRD, and TEM. Subsequently, an assessment was conducted to determine the minimum inhibitory concentration (MIC) of Ag-NPs and Melittin. Furthermore, the potential synergistic effects of Ag-NPs and Melittin with ineffective antibiotics were assessed. By applying the following equation to the Fractional Inhibitory Concentration Index (FICI) value .

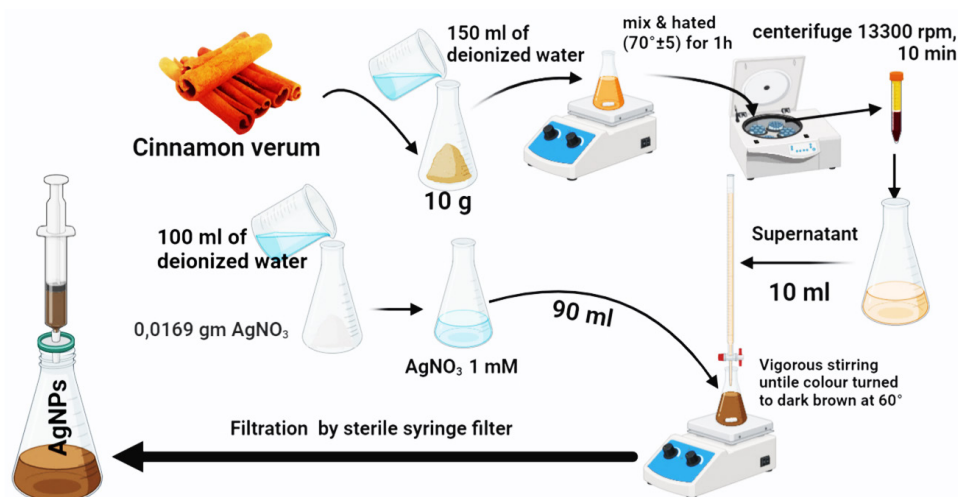
$$FICI = \frac{\text{Growth inhibition of Ab} + \text{Growth inhibition of AgNPs or Melittin}}{\text{Combinations growth inhibition}}$$

FICI considered synergy when  $FICI \leq 0.5$ , partial synergy when  $0.5 < FICI$ , additive when  $FICI = 1$ , effective when  $1 < FICI < 4$ , and antagonism  $1 > 4$ . (Hassan *et al.*, 2021; Tawfeeq *et al.*, 2017).

The equation below was applied to

a 96-well microtiter plate indicator of the color change of resazurin stain in a checkerboard assay to estimate the synergistic state between Melittin and Ag-NPs (Lagatolla *et al.*, 2022).

$$FICI = \frac{MIC \text{ of Colistin in combination}}{MIC \text{ of Colistin alone}} + \frac{MIC \text{ of Ag-NPs in combination}}{MIC \text{ of Ag-NPs alone}}$$



Figure(1): Schematic diagram depicting the biosynthesis process of Ag-NPs

## 4- Results:

### 4-1 Sample collection and diagnosis:

A total of 255 stool samples were acquired from persons suffering from diarrhoea, comprising both male and female patients ranging in age from six months to 72 years. A comprehensive analysis was conducted on a total of 120 samples to determine the presence of bacterial infection, resulting in a prevalence rate of 47.06%. The determination of the distribution of these samples was accomplished using biochemical and confirmatory studies uti-

lizing the Vitek2 compact, as illustrated in the accompanying chart.

### 4-2: Biosynthesis of Silver nanoparticles.

The efficacy of silver ion-reducing biocomposites in cinnamon bark extract was demonstrated by the precise colour change of a colourless  $\text{AgNO}_3$  solution to a dark brown colour, indicating the conversion of  $\text{Ag}^+$  ions into nanosilver  $\text{Ag}^0$ . This outcome, depicted in Figure(2), highlights the successful green biosynthesis process (Mohammed & Hawar, 2022).

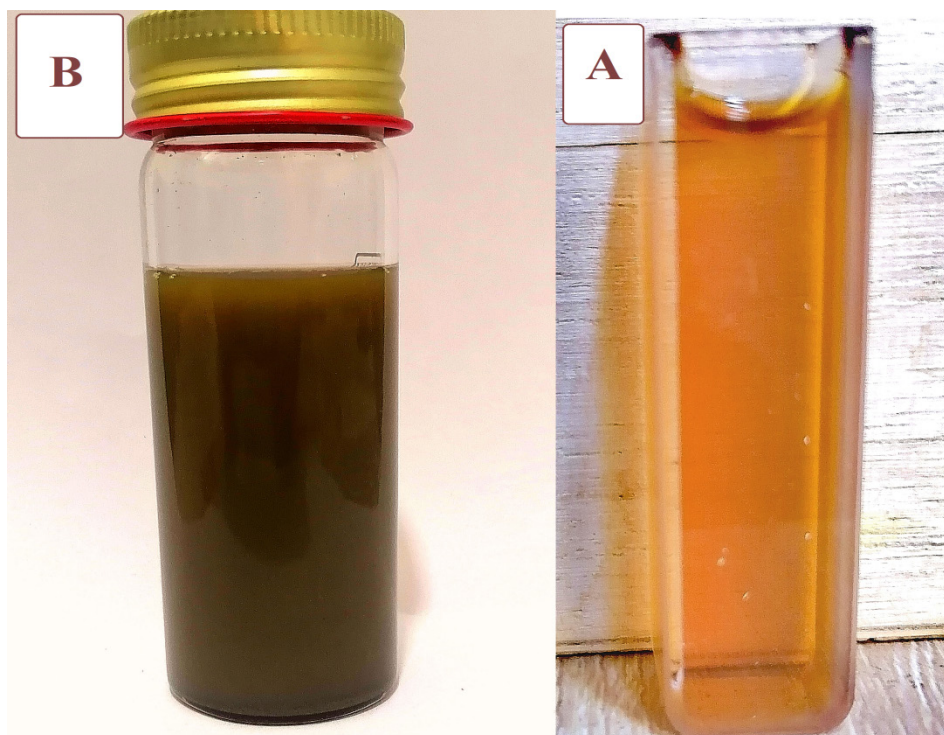


Figure (2) (A) Cinnamon verum extract, (B) Ag-NPs deep brown

### 4-3: UV- Vis spectroscopy.

AgNP synthesis was confirmed by UV-Vis spectroscopy analysis on both the cinnamon plant extract and the nano solution. The resulting standard curves of UV absorption, depicted in Figure (3), indicated the presence of two peaks at 220 nm, 312 nm, and 429

nm for the synthesised silver nanoparticles, which corresponded to the synthesised silver nanoparticles. The test results show concurrence with prior research, wherein the bark of the cinnamon plant was employed as a reducing agent for metallic silver ions (Al-Saeed & Alwan, 2021).

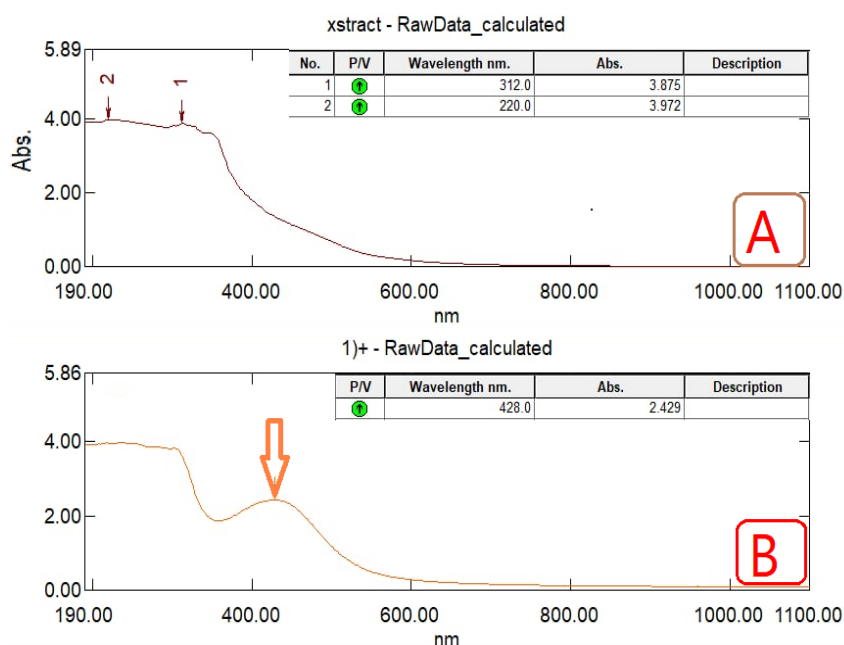


Figure (3): UV-visible spectroscopy, (A) Cinnamon verum extract, (B) Ag-NPs

### 4-4: FT- IR

The results of the FTIR technique, as depicted in Figure(4), demonstrated the spectral range of 400-4000  $\text{cm}^{-1}$  for silver nanoparticles that were reduced using cinnamon bark extract. The analysis revealed the presence of numerous active biomolecules, with

phenols being represented by the carboxyl group ( $-\text{OH}$ ) at  $3587 \text{ cm}^{-1}$  and the carbonyl group ( $\text{C}=\text{O}$ ) at  $1747 \text{ cm}^{-1}$ . Furthermore, the frequency range of  $1577 \text{ cm}^{-1}$  indicated the existence of aromatic compounds ( $\text{C}-\text{C}$ ), while the wave number of  $1539 \text{ cm}^{-1}$  suggested the presence of organic nitro com-

pounds. Additionally, the fingerprinting region exhibited the occurrence of various organic compounds, including aliphatic amine (C-N) groups, (C-N)

groups, and the chemical bond (C-O) associated with amino groups (KGaA, 2020).

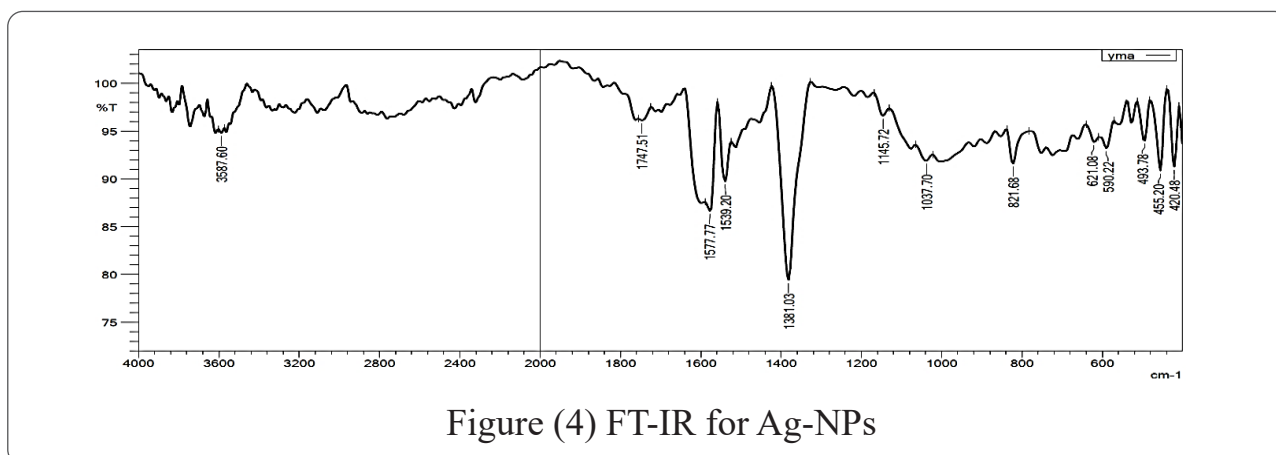


Figure (4) FT-IR for Ag-NPs

#### 4-5: X-ray diffraction (XRD).

The X-ray diffraction (XRD) analysis of the nanoparticles provides a precise assessment of their crystalline structural characteristics. The examination revealed the presence of four distinct peaks (at 38.45, 44.65, 64.90,

and 77.80 degrees) within the 2 Theta angular range, which corresponds to the crystallographic plane labelled as Ag - Card number [00-004 -0783]. The observed peaks in Figure(5) indicate a cubic shape for the nanoparticles (Swanson, 1953).

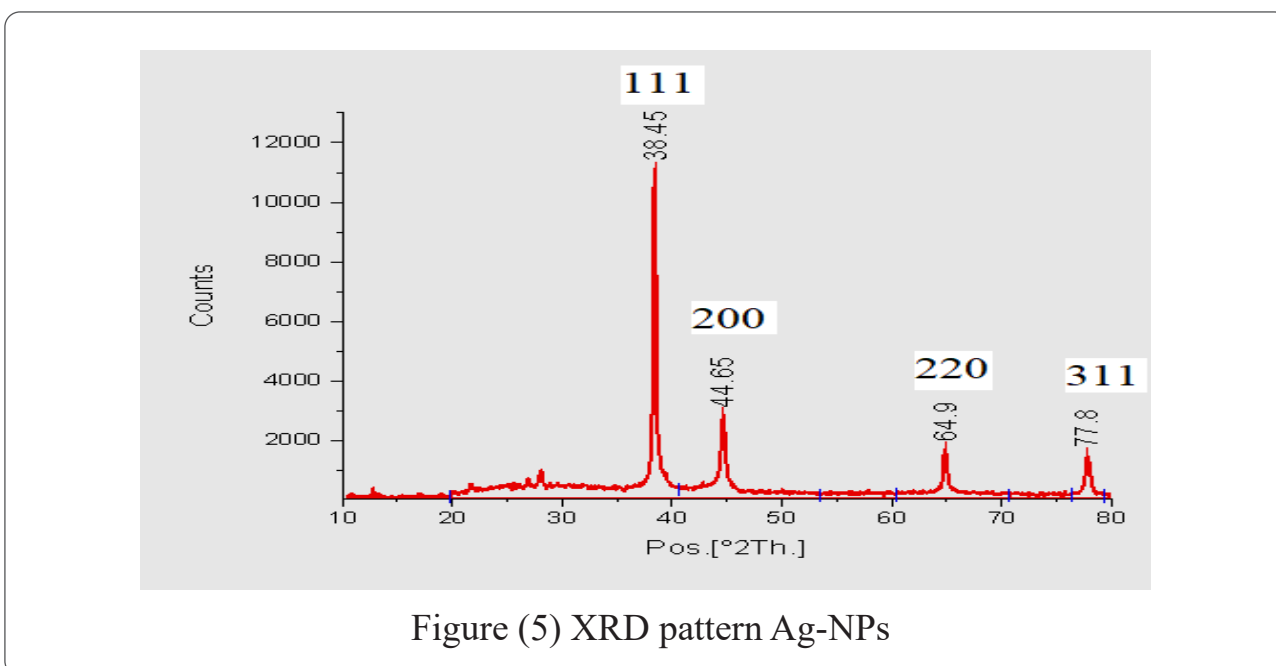


Figure (5) XRD pattern Ag-NPs

Based on the data provided in Table 1, the application of Scherrer's equation yielded an average crystalline size of 20.35 nm for the silver nanoparticles.

Peak position	FWHM	Size of Ag-NPs
38.45	0.35256	23.85468848
44.6501	0.46261	18.55703481
64.9043	0.44877	20.97017253
77.8021	0.56605	18.02694709
	Average	20.35221073

#### 4-6: Transmission electron microscope (TEM).

In Figure(6), TEM images display a surface model of silver nanopar-

ticles (Ag-NPs) with a mainly spherical shape. The observed Ag-NPs possess varying sizes, ranging from 8.13 to 54.11 nm. with an average of 22.81

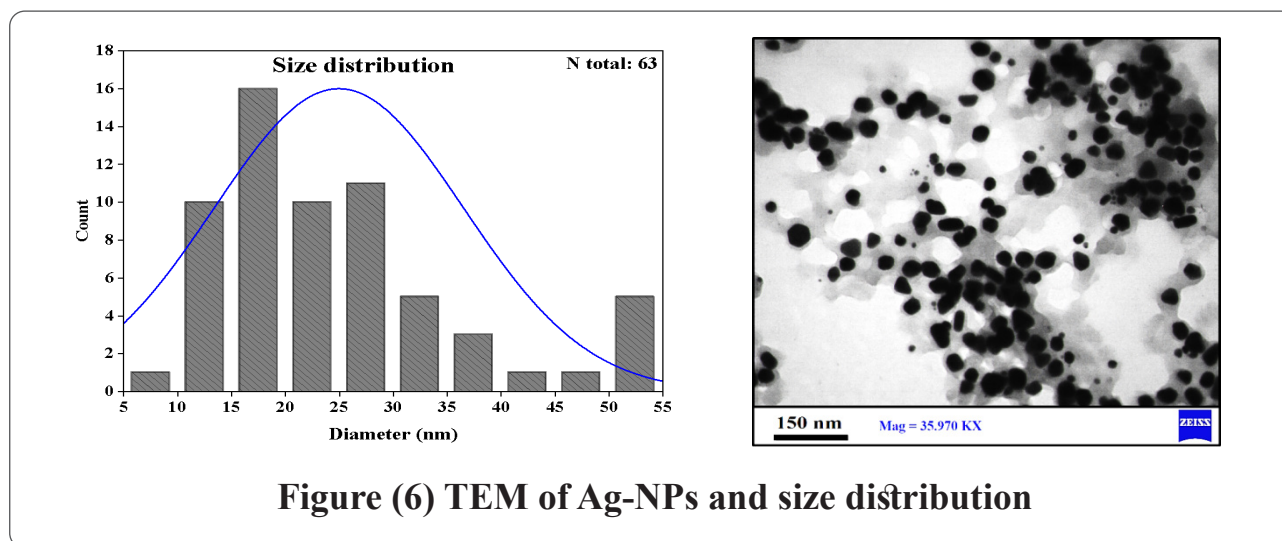


Figure (6) TEM of Ag-NPs and size distribution

The results obtained from Figure (7) of the Energy Dispersive Spectroscopy (EDS) test revealed the identification and quantification of chemical elements and minerals, along with an estimation of their relative abundance. Specifically, the analysis indicated the presence of the chemical element sil-

ver, which accounted for 94.6% of the total weight percentage. The highest intensity peak in the obtained spectrum was observed at an energy level of 3 KeV. In contrast, the presence of the oxygen element was observed at a relatively modest proportion of 5.4%.

The significant prevalence of sil-

ver synthesis can be attributed to the remarkable biosynthetic efficacy and efficiency of biomolecules present in

Cinnamon bark extract, which possess the ability to reduce and create Ag-NPs.

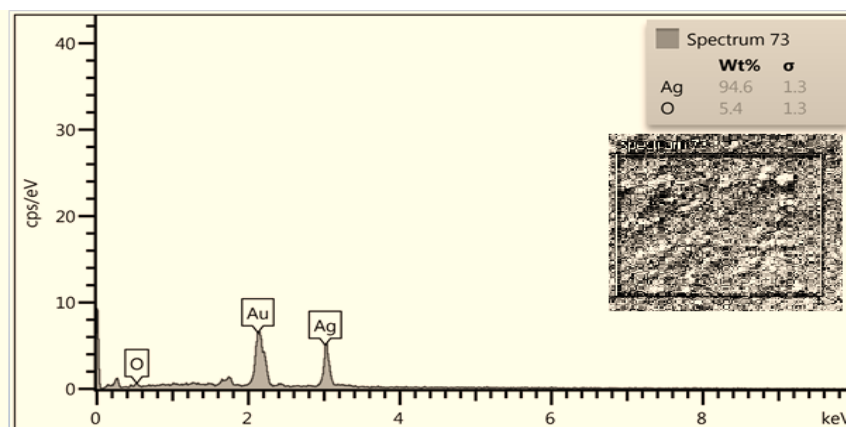


Figure (7) EDS test for prepared Ag-NPs

#### 4-8: Investigation of antibiotic resistance of bacterial isolates.

The resistance patterns of the bacterial isolates analysed for the selected antibiotics commonly associated with bacterial-induced diarrheal disease are presented in Table 1. The results indicate that there was a presence of ampicillin resistance in *E. coli*, *Salmonella* spp, and *Enterococcus* spp, with resistance rates of 76.6%, 71.4%, and 69.2% respectively. As previously stated, the isolates demonstrated differing degrees of resistance to Ceftriaxone, with resistance proportions recorded at 51.6%, 35.7%, and 46.2%, respectively. The isolates of *Escherichia coli*,

*Salmonella* species, and *Staphylococcus* species showed relatively low levels of resistance to Gentamicin, with resistance percentages of 15.6%, 7.1%, and 37.5% respectively. The resistance rates for *E.coli* and *Salmonella* spp. were found to be relatively low for Amikacin, at 4.7% and 0% respectively. Variation in resistance to ciprofloxacin was observed across different species, with around 50% of the isolates, specifically *Salmonella* and *Staphylococcus* spp, displaying resistance to this particular antibiotic. On the other hand, the rates of resistance for *E.coli* and *Enterococcus* spp were found to be 29.7% and 23%, respectively. The spe-

cies chosen for this investigation exhibited a high level of resistance to Trimethoprim, with recorded percentages of 61%, 71.4%, and 62.5% for *E.coli*, *Salmonella*, and *Staphylococcus spp.*, respectively. The resistance rates to tetracycline varied between 57.1% and 50% among multiple bacterial species, except for *Enterococcus spp.*, which

displayed a resistance rate of 38.5%.

Two types of Gram-positive bacteria, specifically *Staphylococcus* and *Enterococcus* species, were also recorded. The observed resistance rates for erythromycin were 87.5% and 76.5% for the respective species, whereas the resistance rates for vancomycin were 37.5% and 23%.

Table (1): Percentages of antibiotic resistance

	<i>E.coli</i> (64)	<i>Staphylococcus spp</i> (8)
	R (%)	R (%)
<b>Ampicillin</b>	49(76.6%)	_____
<b>Ceftriaxone</b>	33(51.6%)	_____
<b>Gentamicin</b>	10(15.6%)	3(37.5%)
<b>Amikacin</b>	3(4.7%)	_____
<b>Ciprofloxacin</b>	19(29.7%)	4(50%)
<b>Trimethoprim</b>	39(61%)	5(62.5%)
<b>Tetracycline</b>	36(56.2%)	4(50%)
<b>Erythromycin</b>	_____	7(87.5%)
<b>Vancomycin</b>	_____	3(37.5%)MIC

#### 4-9: Antimicrobial activity of Ag-NPs and Melittin.

According to their respective minimum inhibitory concentration (MIC) values, Table 2 shows the efficacy of

Ag-NPs and Melittin on the chosen bacterial isolates. Subsequently, these concentrations are utilized to determine the inhibitory zone diameter, as depicted in Figure 8, 9.

**Table (2): Antimicrobial activity of Ag-NPs & Melittin**

Bacteria	Ag-NPs		Melittin	
	MIC( $\mu\text{g/ml}$ )	IZ(Mm)	MIC( $\mu\text{g/ml}$ )	IZ(Mm)
<i>Escherichia coli</i>	5	12	32	12
<i>Staphylococcus aureus</i>	10	15	8	13

MIC: minimum inhibitory concentration.  $\mu\text{g/ml}$  :microgram\ ml .

IZ: inhibition zone. mm: millimetre

The minimum inhibitory concentration (MIC) for both *E. coli* was shown to be 32  $\mu\text{g/ml}$ , resulting in a halo with a diameter of 12 mm. Similarly, the MIC for *S. aureus* was found to be 8  $\mu\text{g/ml}$ , leading to a halo with a diameter of 13 mm. In general, it has been observed that the antimicrobial activity of silver nanoparticles (Ag-NPs) is more pronounced against Gram-negative bacteria compared to Gram-positive bacteria. This observation is based on the determination of MIC values and the measurement of growth inhibition halo diameter. The differential susceptibility can be attributed to the structural disparity in the cell wall composition. Gram-positive bacteria possess an outer layer of peptidoglycan with a thickness of approximately 30 nm, whereas Gram-negative bacteria have a thinner peptidoglycan layer of about 4 nm (Aljeldah et al., 2022). The differential effective-

ness of silver nanoparticles (Ag-NPs) synthesized using cinnamon bark extract, in comparison to those obtained from alternative biological origins (such as plants or microorganisms), can be ascribed to the complex interaction of several elements. The shape and size of nanoparticles are significant characteristics that have a major impact, as toxicity levels demonstrate an inverse correlation with particle size. There is a positive correlation between the effectiveness of granules and their smaller size, whereby smaller granules exhibit a higher effectiveness rate. Moreover, granules exhibiting a spherical morphology or a close approximation exhibit an augmented surface area, enhancing the interaction probability between the nanoparticles' most extensive surface region and cellular membranes. As a result, these granules, which are spherical or spherical-like in shape, demon-

strate superior efficacy in comparison to other manufactured shapes that exhibit transparency (Adebayo-Tayo *et al.*, 2019). TEM exhibited a distinct circular morphology, (XRD) examination revealed the presence of a cubic crystal-line structure; moreover, the utilization of the Shearer equation yielded relatively diminutive crystal sizes, (EDS) investigation results indicated a significant concentration of silver, and it was observed that biomolecules were present alongside the nanomaterials, serving as capping agents and ensuring the stability and dispersion of the nanomaterials, thereby inhibiting their aggregation.

Table 2 presents the findings indicating the efficacy of Melittin against *E. coli* as demonstrated by MIC values of 32  $\mu\text{g/ml}$  and the corresponding inhibition

zones of 12mm. Nevertheless, it should be noted that *S. aureus* exhibit more susceptible to Melittin, as seen by MIC of 8  $\mu\text{g/ml}$  and inhibition zones of 13 mm.

The apparent results of Melittin peptide activity showed that the concentration needed to inhibit the growth of Gram-negative bacteria is relatively higher than that used to eliminate Gram-positive bacteria. This may be attributed to structural differences in the composition of the cell wall, as Melittin can penetrate the peptidoglycan layer and reach the cell membrane easily. At the same time, gram-negative bacteria protect their plasma membrane with a cell wall containing an outer layer of lipopolysaccharides (Galdiero *et al.*, 2019).

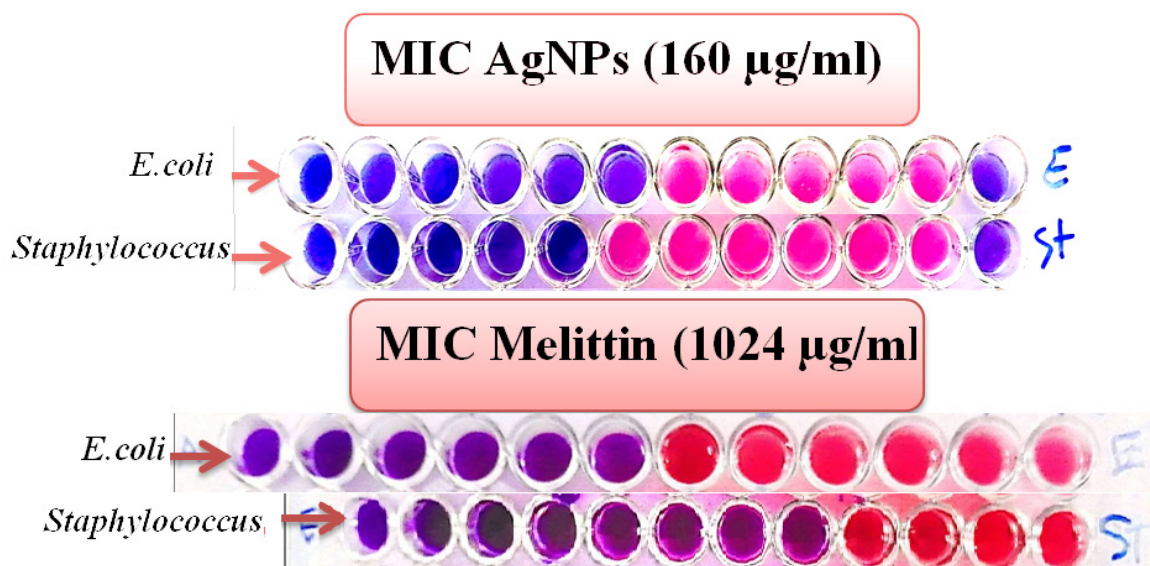


Figure (8): MIC for Ag-NPs & Melittin

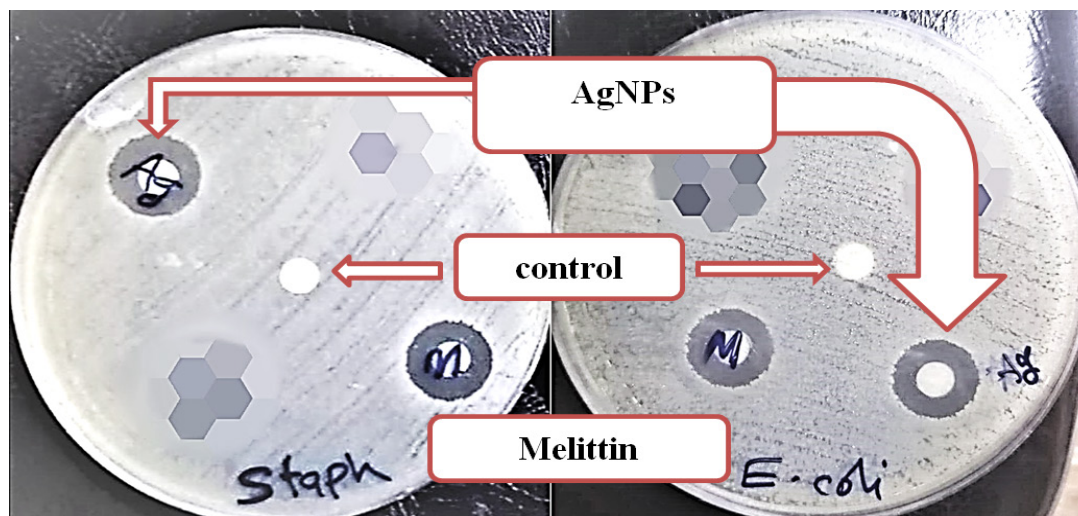


Figure (9): Inhibition zone of Melittin& Ag-NPs

#### 4-10: Synergistic efficacy of Ag-NPs and melittin with antibiotics.

Table(3,4) presents the observed synergistic effect between Ag-NPs and Melittin when combined with antibiotic discs that were previously assessed and shown to be ineffective against the bacterial isolates As depicted in Figure 10. Table (3) shows that a partial synergistic effect was observed when Ag-NPs and Melittin were combined with Ceftriaxone and Ciprofloxacin. For *E. coli*, the FICI was (0.74, 0.6). However, no explicit synergistic effect was observed with the other antibiotics. FICI values of 0.6 showed that melittin and ciprofloxacin demonstrated a partial synergy against *E. coli*.

The observed synergistic interaction between Ag-NPs and ceftriaxone can be

attributed to the inhibitory effect of Ag-NPs on bacterial synthesis of extended-spectrum  $\beta$ -lactamases. This makes it possible for ceftriaxone to target and break up the cell wall structure without being affected by enzyme blockers that could make the antibiotic less effective (Mohammed *et al.*, 2021). Moreover, The efficacy of Ag-NPs to their capacity to adhere to the cellular wall and subsequently disrupt the bacterial cell membrane. This disruption is achieved by stimulating cells to release reactive oxygen species (ROS) from free radicals. These ROS exhibit toxic properties against bacteria and contribute to the degradation of essential biomaterials. Various critical components can be found within the cellular environment, including DNA, proteins, and lipids (C. Singh *et al.*, 2023).

**Table(3) The synergistic effectiveness of Ag-NPs and Melittin in combination with antibiotics against *E. coli*.**

<i>E.coli</i>	AM	CTR	GM	AK	CIP	TM	TE
<b>Ab only</b>	0	8	-	-	0	5	-
<b>Ab+ Ag-NPs</b>	12	27	-	-	18	13	-
<b>FICI</b>	1	0.74	-	-	0.6	1.3	-
<b>Effect</b>	Additive	P.synergy	-	-	P.synergy	Non	-
<i>E.coli</i>	AM	CTR	GM	AK	CIP	TM	TE
<b>Ab only</b>	0	8	-	-	0	5	-
<b>Ab+ Melittin</b>	7	20	-	-	20	10	-
<b>FICI.</b>	1.7	1	-	-	0.6	1.7	-
<b>Effect</b>	Non	Additive	-	-	P.synergy	Non	-

**AM: Ampicillin, CTR: Ceftriaxone, GM: Gentamycin, AK: Amikacin, CIP: Ciprofloxacin, TM: Trimethoprim, TE: Tetracycline**

The results presented in Table (4) demonstrate the interaction between vancomycin and tetracycline in the presence of Ag-NPs, specifically in the partial synergy mode. The FICI values obtained for *S. aureus* were 0.8 and 0.52, respectively. In contrast, the

remaining antibiotics did not exhibit any evident instances of synergy. Also, a study found that Melittin with vancomycin and tetracycline worked well against *S. aureus*, with a FICI of 0.72, 0.81 respectively.

**Table (4) The synergistic effectiveness of Ag-NPs and Melittin in combination with antibiotics against *S. aureus* .**

<i>S.aureus</i>	AM	VA	E	TE	CIP	TM
<b>Ab only</b>	14	8	0	0	-	5
<b>Ab+ Ag-NPs</b>	20	26	7	29	-	15
<b>FICI</b>	1.45	0.8	1.74	0.52	-	1.33
<b>Effect</b>	Non	P.synergy	Non	P.synergy	-	Non
<i>S.aureus</i>	AM	VA	E	TE	CIP	TM
<b>Ab only</b>	14	8	0	0	-	5
<b>Ab+ Melittin</b>	20	29	8	16	-	11
<b>.FICI4</b>	1.35	0.72	1.62	0.81	-	1.63
<b>Effect</b>	Non	P.synergy	Non	P.synergy	-	Non

**AM: Ampicillin, VA: Vancomycin, E: Erythromycin, TE: Tetracycline, CIP: Ciprofloxacin, TM: Trimethoprim,**

The small size of melittin and its high ability to break down biological membranes, such as cytoplasmic membranes, by creating pores and destroying the structure of the cytoplasmic membrane of bacterial cells gives the peptide the possibility of cooperating

with some antibiotics with different mechanisms, whether they target the cell wall, such as Ceftriaxone, or others that attack the internal organelles of bacteria, such as Ciprofloxacin, which targets enzymes that regulate the structure of DNA.

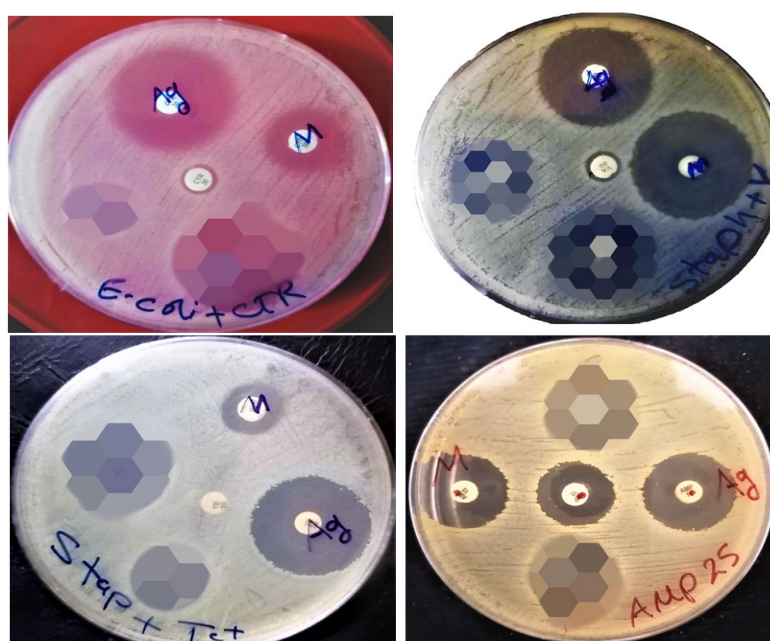


Figure (10): synergism pattern of Melittin and Ag-NPs with antibiotics

**4-11: Synergistic interaction of melittin with Ag-NPs.**

The findings depicted in Table (5) illustrate a distinct, synergistic effect

between melittin and Ag-NPs. FICI values obtained for the bacterial strains *E. coli* and *S. aureus* were 0.37, 0.24 respectively.

Table (4): The synergistic effect of combining melittin and Ag-NPs.

	<i>E.coli</i>	<i>S. aureus</i>
<b>Melittin alone</b>	32	8
<b>Synergistic melittin</b>	8	1
<b>AgNP alone</b>	5	10
<b>Synergistic of AgNP</b>	0.62	1.25
<b>FICI</b>	0.37	0.24
<b>Effect</b>	synergy	Synergy

The synergistic interaction between melittin peptide and AgNPs can be attributed to the antimicrobial properties of silver nanoparticles. When AgNPs release silver ions ( $\text{Ag}^+$ ) on the cell surface, they disrupt the components of the cell wall, leading to the formation of pits inside the cell wall (Yin et al., 2020). This creates an opportunity for melittin to penetrate the cell and reach

the cytoplasmic membrane. Two key factors contribute to this process: the relatively small size of melittin, which is composed of 26 amino acids, and its positive charge of (+6). The positive charge of melittin enhances its attraction to negatively charged biological membranes, allowing it to carry out its analytical function and form trans-membrane pores (Hong *et al.*, 2019).

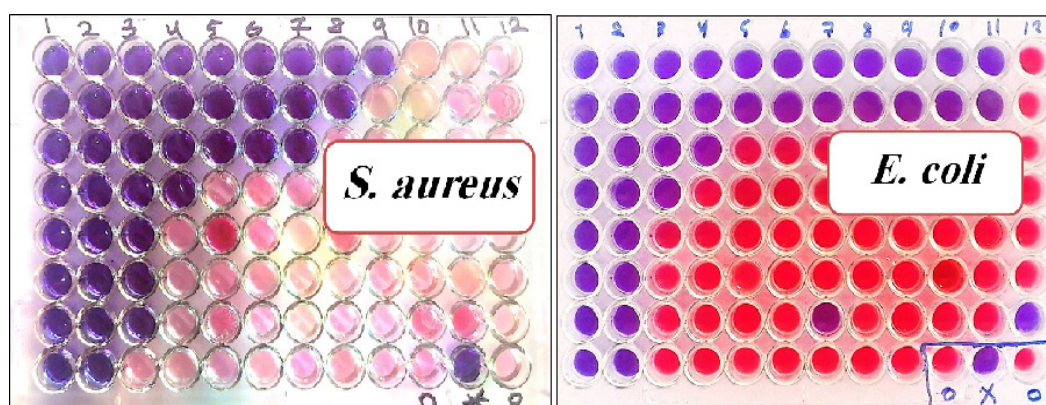


Figure (11) : Checkerboard assay for Melittin and Ag-NPs

### Conclusions

The information presented led to the observation that the production of silver nanoparticles could be effectively achieved using a green biological technique that included cinnamon bark extract. Melittin and Ag-NPs have both shown antibacterial properties by successfully preventing the growth of

germs. Moreover, they have shown synergistic benefits in combination with ceftriaxone, ciprofloxacin, vancomycin, and tetracycline, among other antibiotics. It has been shown that the effectiveness of melittin against Gram-positive bacteria is greater than that of Gram-negative bacteria.

## REFERENCES

1. Abdurrahman, G., Schmiedeke, F., Bachert, C., Bröker, B. M., & Holtfreter, S. (2020). Allergy—a new role for T cell superantigens of *Staphylococcus aureus*? *Toxins*, *12*(3), 176.
2. Adebayo-Tayo, B., Salaam, A., & Ajibade, A. (2019). Green synthesis of silver nanoparticle using *Oscillatoria* sp. extract, its antibacterial, antibiofilm potential and cytotoxicity activity. *Heliyon*, *5*(10), e02502.
3. Al-Dahmoshi, H. O., Rabeea, H. W., Aridhee, A. S. A., Al-Khafaji, N. S., Al-Allak, M. H., Lazm, A. M., & Jebur, M. S. (2019). Phenotypic investigation of vancomycin, teicoplanin and linezolid resistance among *Enterococcus* spp. isolated from children diarrhea. *J Pure Appl Microbiol*, *13*(1), 531-536.
4. Aljeldah, M. M., Yassin, M. T., Mostafa, A. A.-F., & Aboul-Soud, M. A. (2022). Synergistic Antibacterial Potential of Greenly Synthesized Silver Nanoparticles with Fosfomycin Against Some Nosocomial Bacterial Pathogens. *Infection and drug resistance*, 125-142.
5. Al-Saeed, M., & Alwan, S. (2021). Biosynthesized silver nanoparticles (using *Cinnamomum zeylanicum* bark extract) improve the fertility status of rats with polycystic ovarian syndrome. *Biocatalysis and Agricultural Biotechnology*, *38*, 102217. <https://doi.org/10.1016/j.bcab.2021.102217>
6. Alwan, S. H., & Al-Saeed, M. H. (2021). Biosynthesized silver nanoparticles (using *Cinnamomum zeylanicum* bark extract) improve the fertility status of rats with polycystic ovarian syndrome. *Biocatalysis and Agricultural Biotechnology*, *38*, 102217.
7. Anbazhagan, A. N., Priyamvada, S., Alrefai, W. A., & Dudeja, P. K. (2018). Pathophysiology of IBD associated diarrhea. *Tissue barriers*, *6*(2), e1463897.
8. Batool, A., Bore, M., Wu, J., Li, C., & Zeng, H. (2023). Augmented antibacterial activity of cefazolin with silver nanoparticles against *Staphylococcus aureus* and *Escherichia coli*. *Journal of Drug Delivery Science and Technology*, *85*, 104550. <https://doi.org/https://doi.org/10.1016/j.jddst.2023.104550>
9. Chu, C., Rotondo-Trivette, S., &

- Michail, S. (2020). Chronic diarrhea. *Current Problems in Pediatric and Adolescent Health Care*, 50(8), 100841.
10. Deichsel, E. L., Keita, A. M., Verani, J. R., Powell, H., Jamka, L. P., Hossain, M. J., Jones, J. C. M., Omoro, R., Awuor, A. O., & Sow, S. O. (2023). Management of diarrhea in young children in sub-Saharan Africa: adherence to World Health Organization recommendations during the global enteric multisite study (2007–2011) and the Vaccine Impact of Diarrhea in Africa (VIDA) Study (2015–2018). *Clinical Infectious Diseases*, 76(Supplement\_1), S23-S31.
11. Depta, J., & Niedźwiedzka-Ryśwejt, P. (2023). The Phenomenon of Antibiotic Resistance in the Polar Regions: An Overview of the Global Problem. *Infection and drug resistance*, 1979-1995.
12. Dey, S., Gaur, M., Sykes, E. M., Prusty, M., Elangovan, S., Dixit, S., Pati, S., Kumar, A., & Subudhi, E. (2023). Unravelling the Evolutionary Dynamics of High-Risk *Klebsiella pneumoniae* ST147 Clones: Insights from Comparative Pangenome Analysis. *Genes*, 14(5), 1037.
13. do Nascimento, L. G., Fialho, A. M., de Andrade, J. d. S. R., de Assis, R. M. S., & Fumian, T. M. (2022). Human enteric adenovirus F40/41 as a major cause of acute gastroenteritis in children in Brazil, 2018 to 2020. *Scientific reports*, 12(1), 11220.
14. Ehuwa, O., Jaiswal, A. K., & Jaiswal, S. (2021). Salmonella, food safety and food handling practices. *Foods*, 10(5), 907.
15. El-Sayed Ahmed, M. A. E.-G., Zhong, L.-L., Shen, C., Yang, Y., Doi, Y., & Tian, G.-B. (2020). Melittinand its role in the Era of antibiotic resistance: an extended review (2000–2019). *Emerging microbes & infections*, 9(1), 868-885.
16. Hassan, K. T., Ibraheem, I. J., Hassan, O. M., Obaid, A. S., Ali, H. H., Salih, T. A., & Kadhim, M. S. (2021). Facile green synthesis of Ag/AgCl nanoparticles derived from Chara algae extract and evaluating their antibacterial activity and synergistic effect with antibiotics. *Journal of Environmental Chemical Engineering*, 9(4), 105359. <https://doi.org/https://doi.org/10.1016/j.jece.2021.105359>

17. Hong, J., Lu, X., Deng, Z., Xiao, S., Yuan, B., & Yang, K. (2019). How melittin inserts into cell membrane: conformational changes, inter-peptide cooperation, and disturbance on the membrane. *Molecules*, 24(9), 1775.
18. Hossen, M., Gan, S. H., & Khalil, M. (2017). Melittin, a potential natural toxin of crude bee venom: probable future arsenal in the treatment of diabetes mellitus. *Journal of chemistry*, 2017.
19. Huang, H. W. (2006). Molecular mechanism of antimicrobial peptides: the origin of cooperativity. *Biochimica et Biophysica Acta (BBA)-Biomembranes*, 1758(9), 1292-1302.
20. Jarjees, R. K. (2021). Detection of Enterotoxigenic *Staphylococcus aureus* in Patients with Gastroenteritis in Erbil/Iraq. *Indian Journal of Forensic Medicine & Toxicology*, 15(4).
21. Kareem, P. A. (2018). Silver nanoparticles synthesized by using *Matricaria chamomilla* extract and effect on bacteria isolated from dairy products. *Diyala J. Pure Sci*, 14(4), 176-187.
22. Ke, Y., Lu, W., Liu, W., Zhu, P., Chen, Q., & Zhu, Z. (2020). Non-typhoidal *Salmonella* infections among children in a tertiary hospital in Ningbo, Zhejiang, China, 2012–2019. *PLoS neglected tropical diseases*, 14(10), e0008732.
23. KGaA, M. (2020). “ IR spectrum table & chart. URL: <https://www.sigmaaldrich.com/technical-documents/articles/biology/ir-spectrum-table.html>.
24. Kolla, H. B., Tirumalasetty, C., Sreerama, K., & Ayyagari, V. S. (2021). An immunoinformatics approach for the design of a multi-epitope vaccine targeting super antigen TSST-1 of *Staphylococcus aureus*. *Journal of Genetic Engineering and Biotechnology*, 19(1), 1-14.
25. Lagatolla, C., Mehat, J. W., La Ragione, R. M., Luzzati, R., & Di Bella, S. (2022). In Vitro and In Vivo Studies of Oritavancin and Fosfomycin Synergism against Vancomycin-Resistant *Enterococcus faecium*. *Antibiotics*, 11(10), 1334.
26. Li, Y., Xia, S., Jiang, X., Feng, C., Gong, S., Ma, J., Fang, Z., Yin, J., & Yin, Y. (2021). Gut microbiota and diarrhea: an updated review.

- Frontiers in Cellular and Infection Microbiology*, 11, 625210.
27. Liman, S., Bello, Y., Deeni, Y., Lawal, D., & Yahaya, Y. (2023). Molecular Detection of E. coli O157:H 7 Isolated from Infants Diarrheal Stools and Its Sensitivity to *Mangifera indica* (Mango) and *Bosweilia dalzeilii* (Hano) Extracts. *International Journal of Microbiology and Biotechnology*, 30-36. <https://doi.org/10.11648/j.ijmb.20230802.11>
  28. Mariswamy, S. D., Thimmaiah, C. K., Basappachidananda, V. K., Basavaraju, M., & Arkeswaraiah, C. N. (2021). Antimicrobial, haemolytic and antibiofilm assay of green synthesized silver nanoparticles by aqueous extracts of *Rubia cordifolia*. *International Journal of Pharmaceutical Sciences Review and Research*, 28, 174-184.
  29. Mohammad, Z. H., Ahmad, F., Ibrahim, S. A., & Zaidi, S. (2022). Application of nanotechnology in different aspects of the food industry. *Discover Food*, 2(1), 12.
  30. Mohammed, A. S. A., Mourad, M. I., Alsewy, F. Z., & Azzam, N. F. A. E. M. (2021). Combination of silver nanoparticles with ineffective antibiotics against extended spectrum beta-lactamases producing isolates at Alexandria Main University Hospital, Egypt. *Beni-Suef University Journal of Basic and Applied Sciences*, 10, 1-8.
  31. Mohammed, G. M., & Hawar, S. N. (2022). Green Biosynthesis of Silver Nanoparticles from *Moringa oleifera* Leaves and Its Antimicrobial and Cytotoxicity Activities. *International Journal of Biomaterials*, 2022.
  32. Moridi, K., Hemmaty, M., Eidgahi, M. R. A., Najafi, M. F., Zare, H., Ghazvini, K., & Neshani, A. (2020). Construction, cloning, and expression of Melittin antimicrobial peptide using *Pichia pastoris* expression system. *Gene Reports*, 21, 100900.
  33. NEAMAH, B. A. H., & MERZA, F. A. (2023). Investigation of Pathogens that Cause Diarrhea in Children Under 10 Years Old in Al-Najaf Province.
  34. Parvathalu, K., Chinmayee, S., Preethi, B., Swetha, A., Maruthi, G., Pritam, M., Sreenivas, B., Naidu, S. R., Merlinsheeba, G., & Murali, B. (2023). Green synthesis of silver nanoparticles using *Argyrea*

- nervosa leaf extract and their antimicrobial activity. *Plasmonics*, 18(3), 1075-1081.
35. Peter, S. K., Mutiso, J. M., Ngetich, M., Mbae, C., & Kariuki, S. (2023). Seroprevalence of non-typhoidal Salmonella disease and associated factors in children in Mukuru settlement in Nairobi County, Kenya. *PLoS One*, 18(7), e0288015.
36. Pokharel, P., Dhakal, S., & Dozois, C. M. (2023). The diversity of escherichia coli pathotypes and vaccination strategies against this versatile bacterial pathogen. *Microorganisms*, 11(2), 344.
37. Ribeiro, A. I., Vieira, B., Dantas, D., Silva, B., Pinto, E., Cerqueira, F., Silva, R., Remião, F., Padrão, J., & Dias, A. M. (2023). Synergistic Antimicrobial Activity of Silver Nanoparticles with an Emergent Class of Azoimidazoles. *Pharmaceutics*, 15(3), 926.
38. Shrivastava, S. R., Shrivastava, P. S., & Ramasamy, J. (2018). World health organization releases global priority list of antibiotic-resistant bacteria to guide research, discovery, and development of new antibiotics. *Journal of Medical Society*, 32(1), 76-77.
39. Singh, C., Anand, S. K., Upadhyay, R., Pandey, N., Kumar, P., Singh, D., Tiwari, P., Saini, R., Tiwari, K. N., & Mishra, S. K. (2023). Green synthesis of silver nanoparticles by root extract of *Premna integrifolia* L. and evaluation of its cytotoxic and antibacterial activity. *Materials Chemistry and Physics*, 297, 127413.
40. Singh, S., Maurya, P., & Soni, K. (2023). Utilization of Algae for the Green Synthesis of Silver Nanoparticles and Their Applications. *American Journal of Nano Research and Applications*, 11(1), 1-9.
41. Singh, T. A., Singh, T., Boudh, S., & Shukla, P. (2020). Understanding and combating the antibiotic resistance crisis. In *Microorganisms for Sustainable Environment and Health* (pp. 315-328). Elsevier.
42. Swanson, H. E. (1953). Standard X-ray diffraction powder patterns (Vol. 25). US Department of Commerce, National Bureau of Standards.
43. Tawfeeq, S. M. T., Maaroo, M. N., & Al-Ogaidi, I. (2017). Synergistic effect of biosynthesized silver nanoparticles with antibiotics

- against multi-drug resistance bacteria isolated from children with diarrhoea under five years. *Iraqi Journal of Science*, 14-52.
44. Wemyss, M., & Pearson, J. (2019). Host cell death responses to non-typhoidal *Salmonella* infection. *Front Immunol* 10: 1758. In.
45. Zorraquín-Peña, I., Cueva, C., Bartolomé, B., & Moreno-Arribas, M. V. (2020). Silver Nanoparticles against Foodborne Bacteria. Effects at Intestinal Level and Health Limitations. *Microorganisms*, 8, 132. <https://doi.org/10.3390/microorganisms8010132>.
46. Galdiero, E., Siciliano, A., Gesuele, R., Di Onofrio, V., Falanga, A., Maione, A., Liguori, R., Libralato, G., & Guida, M. (2019). Melittin inhibition and eradication activity for resistant polymicrobial biofilm isolated from a dairy industry after disinfection. *International Journal of Microbiology*, 2019.
47. Hong, J., Lu, X., Deng, Z., Xiao, S., Yuan, B., & Yang, K. (2019). How melittin inserts into cell membrane: conformational changes, inter-peptide cooperation, and disturbance on the membrane. *Molecules*, 24(9), 1775.
48. Yin, I. X., Zhang, J., Zhao, I. S., Mei, M. L., Li, Q., & Chu, C. H. (2020). The antibacterial mechanism of silver nanoparticles and its application in dentistry. *International Journal of Nanomedicine*, 2555-2562.
49. Hong, J., Lu, X., Deng, Z., Xiao, S., Yuan, B., & Yang, K. (2019). How melittin inserts into cell membrane: conformational changes, inter-peptide cooperation, and disturbance on the membrane. *Molecules*, 24(9), 1775.

